*Acta Oceanol. Sin.*, 2026, Vol. 45, No. 6, P. 1–14
https://doi.org/10.1007/s13131-025-2621-y

# Effects of stand age on vegetation carbon storage and its spatial distribution of *Aegiceras corniculatum* in the Maowei Sea

Xiaowen Xie[1, 2], Riming Wang[1*], Xiaokui Xie[1], Chunmei Huang[1], Xuxiang Zhang[1], Xuefei Mei[3], Zhijun Dai[1, 2, 3*]

[1] Guangxi Key Laboratory of Marine Environmental Change and Disaster in Beibu Gulf, Beibu Gulf University, Qinzhou 535011, China

[2] Key Laboratory of Environment Change and Resources Use in Beibu Gulf, Ministry of Education, Nanning Normal University, Nanning 530001, China

[3] State Key Laboratory of Estuarine and Coastal Research, East China Normal University, Shanghai 200241, China

Received 9 October 2025; accepted 5 February 2026



## Abstract

Vegetation carbon storage in mangroves is an important component of the global carbon cycle, and its spatial distribution plays a key role in the assessment of coastal blue carbon storage. However, there are substantial differences in vegetation carbon storage among mangroves of different ages, introducing uncertainties into blue carbon assessments. In this study, field samples of young, middle-aged, and mature *Aegiceras corniculatum* from the Maowei Sea (MWS) were integrated with remote sensing imagery to investigate the effect of stand age on vegetation carbon storage and its spatial distribution in *A. corniculatum*. The results indicated that the carbon content in different organs of young *A. corniculatum* followed the pattern stem > leaf > root, whereas in middle-aged and mature stands it shifted to leaf > stem > root. Across all stand ages, carbon storage among organs in *A. corniculatum* consistently followed the pattern stem > root > leaf. Meanwhile, the carbon storage of *A. corniculatum* increased significantly with age. The carbon storage of individual trees was (50.57 ± 10.13) g, (4 837.69 ± 1 234.03) g, and (6 534.07 ± 874.59) g for young, middle-aged, and mature stages, respectively. The total vegetation carbon storage of *A. corniculatum* in the MWS was 47 829.97 t. Young, middle-aged, and mature stands accounted for 0.39%, 49.37%, and 50.24% of the total storage, respectively, with vegetation carbon densities of (2.28 ± 0.93) t/hm$^2$, (52.04 ± 7.75) t/hm$^2$, and (56.49 ± 12.57) t/hm$^2$. Moreover, the introduction of *Sonneratia apetala* and human disturbance resulted in lower coverage of *A. corniculatum* in the Maoling River Estuary (MRE) but higher coverage in the Qinjiang River Estuary (QRE), leading to a spatial distribution of vegetation carbon storage in the MWS characterized by higher values in the east and lower values in the west. This study reveals the differences in vegetation carbon storage in *A. corniculatum* across ages, providing a scientific basis for the sustainable management of mangroves worldwide.

**Key words** vegetation carbon storage, *Aegiceras corniculatum*, Maowei Sea

**Citation** Xie Xiaowen, Wang Riming, Xie Xiaokui, Huang Chunmei, Zhang Xuxiang, Mei Xuefei, Dai Zhijun. 2026. Effects of stand age on vegetation carbon storage and its spatial distribution of *Aegiceras corniculatum* in the Maowei Sea. Acta Oceanologica Sinica, 45(6): 1–14, doi: 10.1007/s13131-025-2621-y

## 1 Introduction

Mangroves, widely distributed in the intertidal zones of tropical and subtropical coasts, are considered a vital component of blue carbon ecosystems due to their high capacity for long-term natural carbon sequestration (Alongi, 2014; Wang et al., 2023; Lovelock and Duarte, 2019). Despite covering a mere 0.5% of the global coastal area, mangroves store a disproportionately high 10%−15% of the carbon sequestered in coastal ecosystems, playing a

Foundation item: The National Natural Science Key Foundation of China under contract Nos 42366009 and 41930537; Shanghai International Science and Technology Cooperation Fund Project under contract Nos 23230713800 and 19230742700.
*Corresponding author, E-mail: wangriming@bbgu.edu.cn; zjdai@sklec.ecnu.edu.cn

significant role in the global carbon cycle (Duarte et al., 2005). However, mangroves are facing the dual threats of human activities and natural factors, leading to severe losses (Thomas et al., 2017). Globally, mangroves are being lost at an annual rate of approximately 0.16%−0.39%, which results in carbon storage losses of up to 2.0−7.5 Tg/a (in terms of C) (Hamilton and Casey, 2016). The vegetation carbon storage of mangroves is more vulnerable to disturbance than soil carbon and exhibits greater interannual variability (Li et al., 2025), posing significant challenges for the accurate estimation of regional carbon storage. Therefore, being concerned about how to accurately evaluate the vegetation carbon storage in mangroves has become a focus of blue carbon research.

Vegetation carbon storage in mangroves is controlled by age, plant density, tree species, human activities, and species invasion (Harishma et al., 2020; Thomas et al., 2017; Lu et al., 2014). Studies have shown that stand age is the main driving factor of vegetation carbon storage in mangroves (Li et al., 2025; Zakaria et al., 2023). Besnard et al. (2025) showed that the vegetation carbon stock in mangroves increases with forest age, with global young mangroves containing 23.80 Mg/hm$^2$ (in terms of C), while old mangroves reach 77.80 Mg/hm$^2$ (in terms of C). Mangroves at different ages adjust the biomass allocation among their organs according to physiological needs, thereby altering the proportion of carbon distributed among these organs (Zhu et al., 2021; Chen et al., 2025). Plant density also plays a critical role in regulating vegetation carbon stock dynamics in mangroves. As succession progresses, the self-thinning process leads to a decrease in plant density, while the accumulation of biomass in surviving individuals drives an increase in carbon storage per unit area (Liao et al., 2025; Bai et al., 2021). In recent decades, anthropogenic activities have had a dramatic effect on the vegetation carbon storage in mangroves (Guo et al., 2024). Song et al. (2023) showed that artificial mangroves planted for 40 years can reach carbon stocks of 127.7 Mg/hm$^2$ (in terms of C), substantially enhancing regional carbon sequestration capacity (Besnard et al., 2025). However, Richards et al. (2020) found that the global carbon stock in mangroves declined by 158.4 Mt over the past two decades due to land cover change. In addition, species invasion poses a threat to the carbon stock of native mangroves. Feng et al. (2025) found that the invasion of *Sonneratia apetala* led to the death of native mangroves, significantly weakening the carbon accumulation capacity of native mangroves. A similar outcome was observed in China and India (Lu et al., 2014; Chakraborty, 2018).

In the early years, researchers primarily relied on field quadrat surveys to develop allometric equations for estimating vegetation biomass, which were then applied to assess carbon storage and analyze its allocation characteristics (Ahmed et al., 2021; Hadi et al., 2019). With the rapid development of remote sensing technology, remote sensing images have been widely used for mangrove mapping and biomass estimation, enabling the assessment of vegetation carbon storage and the monitoring of its dynamics at large spatial scales (Tang et al., 2018; Li et al., 2024; Wang et al., 2025). Existing studies have largely focused on the carbon density of mixed-species forests, carbon allocation patterns among different mangrove species, and the spatiotemporal dynamics and driving factors of carbon storage (Shi et al., 2024; Wu et al., 2022). However, the role of forest age dynamics in species-specific carbon storage remains insufficiently studied.

*Aegiceras corniculatum*, a pioneer mangrove species, is widely distributed in estuarine tidal flats and has a remarkable carbon sequestration capacity (Chen et al., 2021). However, global climate warming and human activities are driving the continued loss of mangrove forests (including *A. corniculatum*), thereby undermining the carbon storage potential of blue carbon ecosystems (Richards et al., 2020). Currently, there is a lack of age-specific quantitative assessments of carbon storage dynamics for this key pioneer species, particularly in the Beibu Gulf, and no similar studies have been reported to date. This knowledge gap constrains our accurate predictions of its recovery trajectories and carbon gains. Therefore, exploring the effects of stand age on vegetation carbon storage and the spatial distribution of *A. corniculatum* not only helps scientifically assess its carbon storage capacity but also provides scientific support for the conservation of blue carbon ecosystems.

Maowei Sea (MWS), located in the northern part of the Beibu Gulf, is characterized by the dominance of *A. corniculatum*. The species covers approximately 46.00% of the total *A. corniculatum* distribution area in the Beibu Gulf (Tao et al., 2017). Therefore, in this study, *A. corniculatum* in the MWS was selected, and field observations were integrated with remote sensing imagery to (1) explore the spatial distribution of vegetation carbon storage in *A. corniculatum* stands at different ages, and (2) evaluate vegetation carbon storage in *A. corniculatum* at different ages in the MWS. The findings will provide a scientific basis for accurately assessing regional blue carbon potential and for guiding mangrove management and ecological restoration efforts.

## 2 Materials and methods

### 2.1 *Study area*

MWS is located in the northern part of the Beibu Gulf in China (Fig. 1a). The region has a southern subtropical monsoon climate, with an annual average temperature of 22.40℃ and an annual average rainfall of 2 150 mm. The tidal regime of this sea area is an irregular diurnal tide, with an average tidal range of 2.50 m (Zhang et al., 2023). As the main inflows into MWS, the Maoling River and Qinjiang River carry large amounts of suspended sediments to the estuary under the combined influence of runoff and tidal currents, forming extensive intertidal mudflats that provide favorable habitat conditions for the growth of local mangrove plants (Kang et al., 2022). The

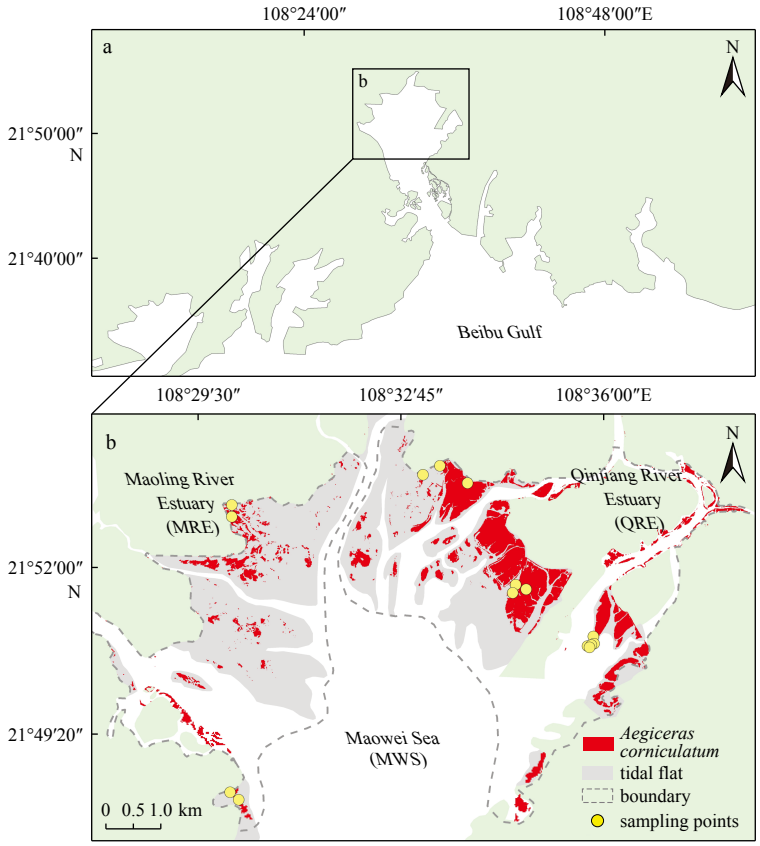


**Fig. 1.** The study area. a. Geographical location of MWS in Guangxi. b. Concentrated distribution area of *A. corniculatum* is divided into QRE and MRE.

mangroves in the MWS are primarily composed of *A. corniculatum, S. apetala*, and *Kandelia obovata*. Since *K. obovata* accounts for only 0.5%, it is excluded from this study (Ma et al., 2019). Based on the geographical distribution of the estuary, this study divided the MWS into the Maoling River Estuary (MRE) and the Qinjiang River Estuary (QRE), aiming to evaluate changes in the vegetation carbon storage of *A. corniculatum* in MWS (Fig. 1b).

### 2.2 *Stand age classification*

Due to their large tree crowns and high canopy density, adult trees typically exhibit a continuous patchy distribution in remote sensing imagery. They possess distinct spectral characteristics that create a significant contrast with other features, making them easy to identify and extract (Chi and Xu, 2025). In contrast, seedlings have smaller crowns, and their spectral characteristics are not distinct in the early stages. Additionally, they are susceptible to spectral interference from features such as tidal flats and herbaceous vegetation, which makes them relatively difficult to identify in remote sensing images. This study used a confusion matrix to evaluate the accuracy of mangrove extraction at different forest ages. When the overall accuracy exceeds 80% and the kappa coefficient is greater than 0.8, the classification results of mangroves of different stand ages can be considered reliable (Hickey and Radford, 2022). Furthermore, during the first five years of growth, mangroves exhibit underdeveloped root and canopy structures, resulting in low resource acquisition efficiency and limited biomass accumulation (Bourgeois et al., 2024). As mangroves grow, stand structure becomes more complete, and photosynthetic nutrient use efficiency improves significantly, thereby promoting rapid biomass accumulation (Sahu and Kathiresan, 2019; Ren et al., 2010). When the stand reaches approximately 20 years of age, the community structure tends to stabilize, biomass growth slows down, and the ecosystem enters the mature stage (Li et al., 2025; Bourgeois et al., 2024). Therefore, based on the growth patterns and remote-sensing detectability of mangroves, this study divided them into three stages: young stands (1−5 a), middle-aged stands (6−19 a), and mature stands (≥ 20 a). Using 2023 as the reference year, young stands were defined as those established between 2019 and 2023, middle-aged stands as those established between 2004 and 2018, and mature stands as those established in or before 2003.

### 2.3 *Extraction of A. corniculatum areas at different ages*

This study used multi-source remote sensing images, combined with field surveys and the 2000−2023 *S. apetala* dataset in the MWS, to quantify the spatial distribution area of *A. corniculatum* across different stand ages. The remote sensing data include 30 m resolution Landsat imagery from 2004, as well as 10 m resolution Sentinel-2 imagery from 2019 and 2023. All selected images met the

criteria of having less than 30% cloud cover and exposed tidal flats, ensuring the completeness of mangrove extraction. To enhance the spectral differentiation between mangroves and other land cover types, Normalized Difference Vegetation Index, Enhanced Vegetation Index, Land Surface Water Index, and Mangrove Vegetation Index indices were further integrated into the imagery. Subsequently, the support vector machine algorithm was applied for mangrove extraction. To improve extraction accuracy and validation, high-resolution QuickBird and WorldView images (0.5−0.6 m resolution) from 2004 and 2019 were used for auxiliary verification (Sentinel-2 imagery was used for 2023). In this study, the overall accuracy exceeded 90% and the Kappa coefficient was greater than 0.90, indicating that the mangrove extraction was highly reliable (Table 1). Since the age classification of *A. corniculatum* is based on multi-temporal mangrove extraction results, the high extraction accuracy provides a reliable guarantee for the age classification of *A. corniculatum*.

To obtain the spatial distribution data of *A. corniculatum*, this study combined field surveys of *A. corniculatum* with the 2000−2023 *S. apetala* dataset for the MWS developed by Xie et al. (2025). Spatial analysis methods such as Intersect and Erase in ArcGIS 10.8 were applied to remove *S. apetala* from the mangrove distribution range in 2004, 2019, and 2023. Through this process, the spatial distribution of *A. corniculatum* was obtained. Finally, the spatial distribution of *A. corniculatum* at different ages was determined through overlay analysis, providing area data support for the subsequent calculation of vegetation carbon storage in *A. corniculatum* at each forest age.

### 2.4 *Vegetation observations and samplings*

Based on the spatial distribution of *A. corniculatum* at different stand ages derived from remote sensing imagery, five survey sites were evenly distributed within the *A. corniculatum* distribution area in MWS for community investigation and sampling. At each survey site, one 5 m × 5 m quadrat was set up in the young, middle-aged, and mature forests, respectively. The total number of plants was counted in each plot, and 10 *A. corniculatum* individuals were selected as sample trees using a five-point sampling pattern. The basal diameter (*D*), diameter at breast height (DBH), and plant height (*H*) of sample trees were measured for the estimation of biomass of *A. corniculatum* at different ages (Table 2) (Fig. 2). Meanwhile, samples of new and old leaves, stems, and roots were collected from the sample trees at each plot, with each sample having a fresh weight of at least 30 g. Subsequently, organs of the same type were mixed to form homogenized composite samples of roots, stems, and leaves, which were used to determine the carbon content of each organ across different stand ages.

**Table 1.** Extraction accuracy

| Time | Overall accuracy/% | Kappa coefficient |
|---|---|---|
| 2004 | 0.96 | 0.95 |
| 2019 | 0.95 | 0.95 |
| 2023 | 0.97 | 0.96 |

**Table 2.** Stand characteristics of *A. corniculatum* at different ages

| Stand ages/a | Plant height/m | Diameter at breast height/cm | Stem diameter/cm | Crown width/cm | Plant density/(stands·hm$^{-2}$) |
|---|---|---|---|---|---|
| Young forests (1−5) | 0.69 | − | 2.09 | 13.11 × 12.93 | 43 800 |
| Middle-agedforests (6−19) | 2.66 | 4.22 | − | 107.21 × 106.14 | 13 900 |
| Mature forests (⩾20) | 3.63 | 9.82 | − | 130.84 × 103.80 | 8 600 |


**Fig. 2.** Measurement of *A. corniculatum*. a. Measurement of diameter at breast height. b. Measurement of plant height.

### 2.5 *Estimation of biomass and vegetation carbon storage*

The allometric equation, as a non-destructive method for estimating biomass, has been widely applied in the estimation of mangrove plant biomass due to its convenience and efficiency (Indrayani et al., 2021). Therefore, this study applied species-specific allometric equations for *A. corniculatum* to estimate its biomass at different ages, providing essential data for the subsequent calculation of vegetation carbon storage. In addition, due to the relatively short height of young forests, their growth characteristics differ significantly from those of middle-aged and mature forests. Using a general allometric equation to estimate the biomass of young forests may result in estimation errors (Hu et al., 2025). Therefore, this study adopted an allometric equation suitable for the young stage of *A. corniculatum* to calculate its biomass, aiming to improve the accuracy of the estimates (Table 3). The allometric equations used in this study were derived from the Beibu Gulf region of China, which shares a high degree of similarity with the study area in terms of latitude, climatic conditions, and species composition. Since these equa-

**Table 3.** Biomass equations for *A. corniculatum* of different ages

| Stand ages | Allometric equation | References |
|---|---|---|
| Young forests | $W_{sb} = 0.011\ 97(D^2H)^{0.885\ 78}$ | Hu et al., 2025 |
| | $W_{lb} = 0.004\ 44(D^2H)^{0.644\ 79}$ | Ning et al., 1996 |
| | $W_{rb} = 0.008\ 4(D^2H)^{0.985\ 8}$ | |
| Middle-aged/Mature forests | Log $AS_W$ = 1.198 + 0.464 Log(DBH$^2H$) | Tam et al., 1995 |
| | Log $AL_W$ = 0.967 + 0.303 Log(DBH$^2H$) | |
| | Log $AB_W$ = 0.393 + 0.475 Log(DBH$^2H$) | |

Note: In the young forests, $W_{sb}$, $W_{lb}$, and $W_{rb}$ indicate the biomass of stems (kg), leaves (kg), and roots (kg), respectively. In the middle-aged and mature forests, $AS_W$, $AB_W$, and $AL_W$ indicate the biomass of stems (kg), leaves (kg), and roots (kg), respectively. $D$, DBH, and $H$ indicate the basal diameter (cm), diameter at breast height (cm), and tree height (m).

tions were developed under similar ecological environments and stand structure conditions, they are considered applicable for accurately estimating the biomass of *A. corniculatum* across different forest ages, thereby ensuring high applicability and reliability in this study.

The collected plant samples of *A. corniculatum* were oven-dried to constant weight and then weighed to obtain their dry weight, which represents plant biomass. Subsequently, the samples were ground and sieved, and the carbon content of each organ across different stand ages was determined using the loss-on-ignition method (He et al., 2018). Thereafter, the carbon storage of the sample tree was calculated using the following formula:

$$C_{st} = c_{root} \times B_{root} + c_{stem} \times B_{stem} + c_{leaf} \times B_{leaf}, \quad (1)$$

where $C_{st}$ is the total carbon storage of the sample tree (kg); $c_{root}$ is the carbon content of the roots (%); $c_{stem}$ is the carbon content of the stems (%); $c_{leaf}$ is the carbon content of the leaves (%); $B_{root}$ is the biomass of roots (kg); $B_{stem}$ is the biomass of stems (kg); and $B_{leaf}$ is the biomass of leaves (kg).

Vegetation carbon density refers to the total amount of carbon stored in the vegetation (including both aboveground parts and roots) per unit area, while plant density represents the number of individuals per unit area and is key parameters for calculating vegetation carbon density. The calculation formula is as follows:

$$PD = \frac{1}{n}\sum_{i=1}^{n}\frac{NP_i}{a_i}, \quad (2)$$

where PD is plant density(stands/hm$^2$); $NP_i$ is the number of plants in the sample plot; $a_i$ is the sample area (hm$^2$); and $n$ is the number of sample plots.

$$C_d = \frac{\sum_{i=1}^{n} C_i N_i}{\sum_{i=1}^{n} a_i}, \quad (3)$$

where $C_d$ is the vegetation carbon density of *A. corniculatum* (t/hm$^2$), $C_i$ is the carbon storage of the sample tree in the $i$-th sample plot (t), $N_i$ is the number of plants in the $i$-th sample plot, $a_i$ is area of the $i$-th sample plot (hm$^2$), and $n$ is the number of sample plots.

The formulas for calculating vegetation carbon storage (including aboveground and root carbon storage) and the total vegetation carbon storage of *A. corniculatum* at different stand ages are as follows:

$$VCS = A \times C_d, \quad (4)$$

where VCS is the carbon storage of different ages (t); and $A$ is the area of *A. corniculatum* in different stand ages (hm$^2$).

$$TVCS = \sum_{i=1}^{3} A_i \times C_d, \quad (5)$$

where TVCS is the total vegetation carbon storage, among them, $i$ = 1 (young forests), 2 (middle-aged forests), 3 (mature forests).

## 3 Results

### 3.1 *Characteristics of carbon content and carbon storage in A. corniculatum*

#### 3.1.1 *Characteristics of carbon content in A. corniculatum*

No significant differences in carbon content were observed among different stand ages of *A. corniculatum* or among its organs (Table 4). Specifically, the carbon content of individual trees ranged from 40.86% ± 2.82% to 44.46% ± 2.20%. The roots had the lowest carbon content, ranging from 38.14% ± 1.25% to 42.00% ± 1.14%. The carbon content of stems and leaves ranged from 41.58% ± 3.40% to 45.24% ± 0.80% and 42.76% ± 3.65% to 45.08% ± 0.84%, respectively.

#### 3.1.2 *Characteristics of carbon storage in A. corniculatum*

Carbon storage of *A. corniculatum* increased with age. There was no significant difference in carbon storage be-

**Table 4.** Carbon content of *A. corniculatum* at different ages

| Stand age | Root/% | Stem/% | Leaf/% | Individual tree/% |
|---|---|---|---|---|
| Young stage | 38.14 ± 1.25a | 45.24 ± 0.80a | 45.08 ± 0.84a | 43.30 ± 0.42a |
| Middle-aged stage | 42.00 ± 1.14a | 44.68 ± 2.51a | 45.00 ± 1.61a | 44.46 ± 2.20a |
| Mature stage | 38.72 ± 2.07a | 41.58 ± 3.40a | 42.76 ± 3.65a | 40.86 ± 2.82a |

Note: Values are presented as mean ± standard error of the mean. Different lowercase letters denote significant differences between values in the same column ($P < 0.05$).

tween the middle-aged and mature stages, but both show significantly higher carbon storage than the young stage (Table 5). Specifically, the carbon storage of an individual tree significantly increased from (50.57 ± 10.13) g/ind. in the young stage to (4 837.69 ± 1 234.03) g/ind. in the middle-aged stage. When the mangrove reached the mature stage, the carbon storage of an individual tree reaches (6 534.07 ± 874.59) g/ind., which is approximately 1.5 times higher than that of the middle-aged stage. The results showed that the most rapid increase of carbon storage occurred between the young and middle-aged stages, and slowed after the middle-aged stage.

With increasing stand age, the carbon storage in each organ showed an increasing trend (Table 5). Carbon storage in all organs was higher in the mature and middle-aged stages than in the young stage, and the order among organs was stem > root > leaf. Further analysis indicated that there are differences in the proportion of carbon storage of each organ to the total carbon storage of an individual plant with increasing stand age. The proportion of carbon storage in the leaves decreased from 18.41% to 5.82%. Meanwhile, the proportion of carbon storage in the stem significantly increased, from 55.78% to 66.77%. The proportion of carbon storage in the roots remained relatively stable, increasing from 25.81% in the young stage to 31.33% in the middle-aged stage, and then decreasing to 27.41% in the mature stage.

### 3.2 *Vegetation carbon density and carbon storage of A. corniculatum*

The vegetation carbon density of *A. corniculatum* followed the pattern: mature forests > middle-aged forests > young forests (Fig. 3A). The vegetation carbon density of the young forests was the lowest, which was only (2.28 ± 0.93) t/hm$^2$, and the middle-aged forests rapidly increased to (52.04 ± 7.75) t/hm$^2$, approximately 23 times higher than that of young forests. The vegetation carbon density of the mature forests increased slightly to (56.49 ± 12.57) t/hm$^2$.

The vegetation carbon storage in young, middle-aged, and mature forests was 186.16 t, 23 611.77 t, and 24 032.04 t, respectively, accounting for 0.39%, 49.37%, and 50.24% of the total vegetation carbon storage (Fig. 3B). Specifically, in the total vegetation carbon storage of

**Table 5.** Carbon storage and its distribution characteristics of *A. corniculatum* at different stand ages

| Stand age | Root/g | Stem/g | Leaf/g | Individual tree/g |
|---|---|---|---|---|
| Young stage | 13.05 ± 2.88b (25.81%) | 28.21 ± 5.89b (55.78%) | 9.31 ± 1.04b (18.41%) | 50.57 ± 10.13b |
| Middle-aged stage | 1 515.82 ± 293.87a (31.33%) | 3 062.65 ± 866.73a (63.31%) | 259.22 ± 74.87a (5.36%) | 4 837.69 ± 1 234.03a |
| Mature stage | 1 791.04 ± 173.18a (27.41%) | 4 362.27 ± 645.90a (66.77%) | 380.77 ± 56.01a (5.82%) | 6 534.07 ± 874.59a |

Note: Values are presented as mean ± standard error of the mean. Different lowercase letters indicate significant differences among values within the same column ($P < 0.05$). Values in parentheses represent the percentage contribution of each organ to the total carbon stock.

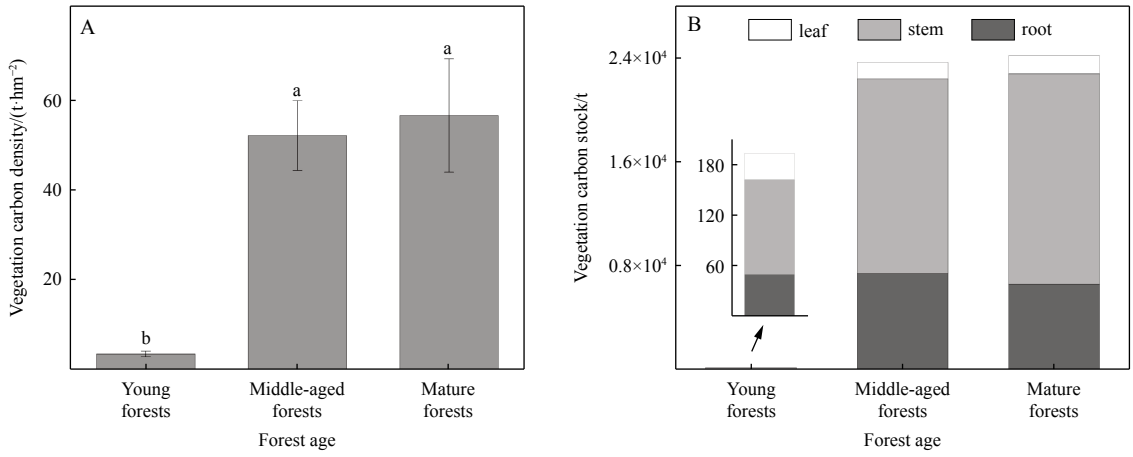


**Fig. 3.** Vegetation carbon density of *A. corniculatum* at different ages (A), carbon storage and allocation characteristics of *A. corniculatum* at different ages (B). Different lowercase letters in Fig. A denote significant differences between values.

the roots, the young, middle-aged, and mature forests accounted for 0.34%, 52.72%, and 46.90%, respectively. In the vegetation carbon storage of the stems, they accounted for 0.35%, 48.07%, and 51.58%, respectively. In the vegetation carbon storage of the leaves, they account for 1.13%, 46.92%, and 51.95%, respectively. Results indicated that the middle-aged and mature forests contributed most to the total vegetation carbon storage of *A. corniculatum*, and that the carbon storage in their roots, stems, and leaves also accounted for relatively high proportions within these organs (Fig. 3B).

### 3.3 *Spatial distribution of vegetation carbon storage in A. corniculatum*

The area of *A. corniculatum* in the MWS was 1 018.43 hm$^2$, with a total vegetation carbon storage of 47 829.97 t, showing a spatial distribution pattern with higher values in the east and lower values in the west (Fig. 4a). The eastern high-value region (QRE) is dominated by mature stands, contributing 53.17% of the total regional carbon stock, while the western low-value region (MRE) is dominated by middle-aged stands, accounting for 64.06% of the regional total (Figs 4b and c).

The area of *A. corniculatum* in the QRE was 825.14 hm$^2$, with vegetation carbon storage of 40 101.66 t, accounting for 83.84% of the total vegetation carbon storage in the MWS. The spatial distribution of vegetation carbon storage exhibited an aggregated pattern, representing a concentrated region for the vegetation carbon storage of *A. corniculatum* in the MWS. In this area, the mature forest covered 377.40 hm$^2$ and hm$^2$s a carbon storage of 21 321.89 t, which exhibited a relatively uniform distribution. The area of the young and middle-aged forests was 358.58 hm$^2$ and 89.16 hm$^2$, with vegetation carbon storage of 119.12 t and 18 660.65 t, respectively. They are mainly concentrated in the central part of the estuary (Fig. 4c). In contrast, the *A. corniculatum* at the MRE covered 193.29 hm$^2$, with the vegetation carbon storage of only 7 728.31 t, exhibiting a fragmented distribution pattern. The areas of young, middle-aged, and mature forests were 50.18 hm$^2$, 95.14 hm$^2$, and 47.97 hm$^2$, respectively, with corresponding carbon storage of 67.04 t, 4 951.12 t, and 2 710.15 t. They were primarily distributed in the northern part of the estuary (Fig. 4b).

## 4 Discussion

### 4.1 *Impact of stand age on carbon storage in A. corniculatum*

The biomass and vegetation carbon storage in mangroves continuously accumulate with growing stand age

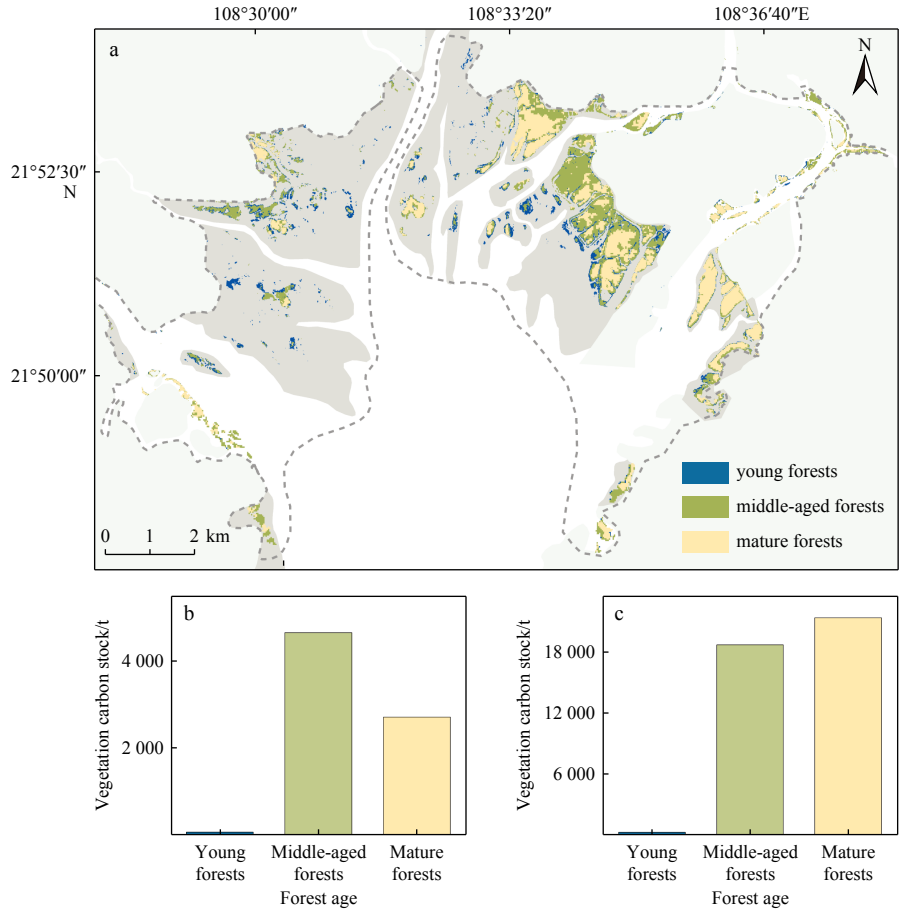


**Fig. 4.** Spatial distribution of vegetation carbon storage in *A. corniculatum* in the MWS (a), vegetation carbon storage of *A.corniculatum* in the MRE (b), vegetation carbon storage of *A. corniculatum* in the QRE (c).

(Song et al., 2024; Conroy et al., 2025). However, studies have shown that the growth rate of vegetation carbon storage in mangrove species such as *K. obovata*, *Avicennia marina*, *S. apetala*, and *Rhizophora stylosa* gradually declines with age (Li et al., 2025; Zheng et al., 2025; Carnell et al., 2022; Ren et al., 2010), which is consistent with the findings for *A. corniculatum* in this study (Fig. 5). In the early growth stage, mangroves experience rapid growth and a swift accumulation of biomass, leading to a fast increase in carbon storage. As biomass gradually stabilizes, the rate of carbon accumulation slows down. However, a decline in the rate of carbon accumulation does not necessarily indicate that mangroves have reached carbon saturation in the short term. Mature mangroves generally have a larger diameter at breast height, greater tree height, and higher canopy height, which hold more biomass (Islam et al., 2023; Rahman et al., 2015; Walcker et al., 2018). Studies have shown that the vegetation carbon storage of mature mangroves worldwide will continue to increase in the coming decades, although the carbon accumulation rate has shown a declining trend (Bourgeois et al., 2024). It suggests that *A. corniculatum* in the MWS maintains a sustained capacity for vegetation carbon storage.

In addition, mangroves adjust their biomass allocation according to their needs at different growth stages, thereby influencing carbon allocation ratios. In the young stage, mangroves typically increase the proportion of leaf biomass to enhance photosynthesis (Simpson et al., 2017). As mangroves develop, biomass gradually concentrates in the stem to enhance structural stability and stress resistance in the harsh intertidal environment, while the proportion of leaf biomass decreases (Yang et al., 2017; Hossain et al., 2016). Chen et al. (2025) confirmed that the proportion of biomass and carbon storage in the stem of mangroves increases with age and remains dominant, while the proportion in the leaves shows a declining trend. Compared with the marked variations in carbon allocation to stems and leaves during individual development, the proportion of carbon allocated to roots remains relatively stable (Table 4). This suggests that carbon allocation in mangrove roots is more susceptible to regulation by environmental factors such as soil salinity, nutrient availability, and tidal dynamics, rather than being solely determined by forest age.

As the forest stands mature, resource competition among plants intensifies, leading to density reduction, and this process is known as self-thinning (Kamara and Kamruzzaman, 2020). Previous studies have shown that during the self-thinning process, the decline in stand density promotes the accumulation of biomass in surviving individuals, thereby enhancing overall vegetation carbon density (Bai et al., 2021; Liao et al., 2025), which is consistent with the results of this study (Fig. 6). In young stands, plants are smaller and have lower demands for resources such as light and nutrients, allowing for a higher stand density per unit area (Rofi'I et al., 2021). However, due to the limited biomass of individual plants, the overall vegetation carbon density remains relatively low. As the stands become mature, limited space and resources intensify intraspecific competition, leading to the mortality of weaker individuals (Liao et al., 2025; Analuddin et al., 2009; Bai et al., 2021). Surviving trees obtain more resources, promoting biomass accumulation and consequently enhancing the vegetation carbon storage of *A. corniculatum*. Higher vegetation carbon density in mature mangroves compared to younger mangroves has also been observed in Bangladesh and Zhejiang Province, China (Islam et al., 2023; Zhou et al., 2025). However, the average vegetation carbon density of *A. corniculatum* in MWS is 36.84 t/hm$^2$, which is 7.85 t/hm$^2$ higher than in China (Liu et al., 2014), but still lower than the global average [(115 ± 7) Mg/hm$^2$, in terms of C] (Kauffman et al., 2020). Compared with other mangrove species worldwide, the vegetation carbon density of the *A. corniculatum* in MWS

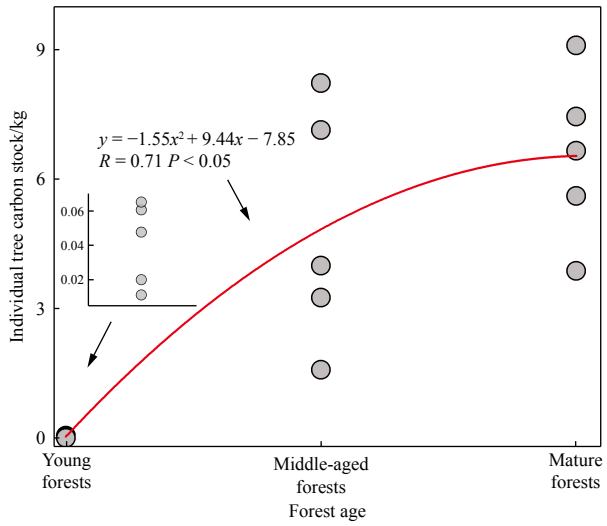


**Fig. 5.** The relationship between carbon storage and age in *A. corniculatum*.

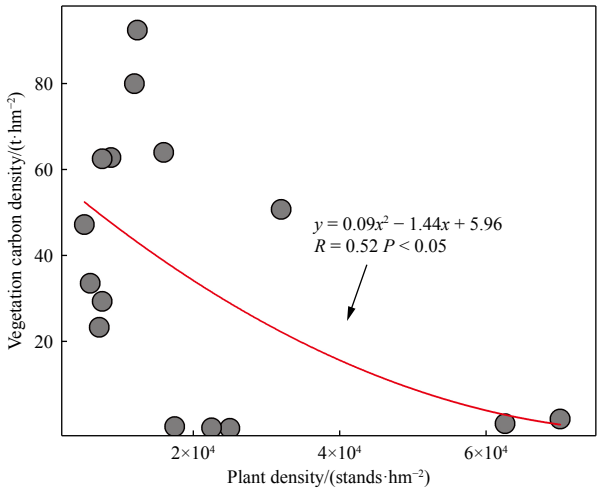


**Fig. 6.** The relationship between plant density and vegetation carbon density in *A. corniculatum*.

is also lower than that of the *Avicennia* [(56.70 ± 9.50) Mg/hm$^2$], *Sonneratia* [(113.30 ± 8.30) Mg/hm$^2$], and *Laguncularia* [(75.20 ± 10.60) Mg/hm$^2$] (Kauffman et al., 2020). It indicates that although the self-thinning process driven by forest age growth promotes carbon accumulation, carbon storage remains constrained by factors such as species characteristics and regional environmental conditions.

### 4.2 *Factors affecting the carbon content of A. corniculatum organs*

The carbon content of *A. corniculatum* and its organs did not significantly vary with stand age in this study. This is consistent with findings from Zhejiang Province, China, which reported no significant differences in the carbon content of the same organs across different ages (5−20 a) of *K. obovata* (Chen et al., 2025). Although forest age had no significant effect on carbon content, significant differences were observed among organs, with stems and leaves exhibiting higher carbon content than roots. Studies have shown that the differences in carbon content among various organs of mangrove plants are closely related to their physiological characteristics and organ functions (Rodrigues et al., 2015; Zheng et al., 2025; Adame et al., 2024). As the main site of photosynthesis, leaves absorb and fix atmospheric $CO_2$ into organic compounds. While some of these compounds accumulate in the leaves, they are also continuously translocated to the stems through the vascular tissue (Perera et al., 2024). Meanwhile, as mangroves grow, stem moisture content gradually decreases while lignification increases, leading to relatively higher carbon content in both the stems and leaves (Liu et al., 2014). In contrast, the root system exhibits lower carbon content, primarily due to the formation of extensive aerenchyma tissue during the development of prop roots, resulting in porous root structures with reduced carbon density (Perera et al., 2024). Moreover, a large number of fine roots with a low degree of lignification are present in the root system, which are prone to carbon release during decomposition, thereby limiting the accumulation of carbon content in the roots (Zheng et al., 2025).

### 4.3 *Anthropogenic activites*

Human activities are important factors influencing mangrove carbon storage and its spatial distribution, leading to the loss of 1.584 Mt of global carbon storage over the past two decades (Dalimunte et al., 2025; Richards et al., 2020; Liu et al., 2024). In the MWS, varying degrees of human disturbance have led to significant differences in the carbon storage of *A. corniculatum* between the QRE and the MRE. Since the 1990s, continuous coastal engineering and the construction of aquaculture ponds in the MRE have greatly weakened the expansion capacity of *A. corniculatum*, resulting in its scattered distribution in the northern part of the estuary and lower carbon storage (Fig. 7a). In contrast, the QRE, which experiences less human disturbance and benefits from nature reserve management, has seen substantial expansion of *A. corniculatum* and enhanced carbon storage capacity (Fig. 7b). Furthermore, the impact of human activities on the carbon storage of *A. corniculatum* is not uniform, and its effects vary with age. Dredging projects carried out after 2010 damaged mangrove tidal flats in the northern and southern parts of the QRE, thereby affecting the regeneration of *A. corniculatum* populations (Fig. 7c). Due to their weaker root anchorage capacity, younger individuals of *A. corniculatum* are more sensitive to habitat disturbances and have difficulty establishing on degraded mudflats, whereas mature stands with well-developed root systems show stronger resistance to external disturbances (Minchinton et al., 2019; Kibler et al., 2022). Consequently, the areas occupied by young and middle-aged stands in the northern and southern estuarine regions are relatively small, resulting in correspondingly lower carbon storage (Fig. 4a).

The artificial introduction of *S. apetala* between 2002 and 2007 exacerbated the disparity in vegetation carbon storage of *A. corniculatum* across the MWS. Early human disturbances weakened the regeneration capacity of *A. corniculatum* populations in the MRE, creating conditions for the invasion of *S. apetala*. After its introduction, it quickly colonized the bare areas and released allelopathic compounds, thereby inhibiting the germination of *A. corniculatum* seeds and the establishment of seedlings, thereby achieving niche pre-emption (Feng et al., 2025; Fazlioglu and Chen, 2020). As *S. apetala* communities developed, their canopies gradually closed, which significantly reduced understory light availability and suppressed the photosynthesis and growth of *A. corniculatum* (Hu et al., 2023; Zhu et al., 2022; Chen et al., 2013) (Fig. 7d). Although mature *A. corniculatum* can maintain relatively

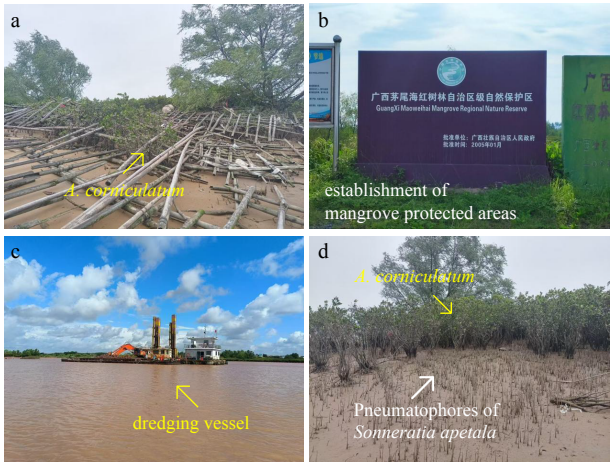


**Fig. 7.** Influence of human activities on *A. corniculatum,* oyster farming destroys *A. corniculatum* (a), establishment of Maowei Sea Mangrove Reserve (b), implementation of the dredging project (c), *Sonneratia apetala* invades the habitat of *A. corniculatum* (d).

high structural stability and resistance in the early stages of competition, prolonged shading and resource competition gradually weaken their physiological activity and growth functions (Peng et al., 2016, 2022; Zhu et al., 2020). Persistent competitive pressure has reduced the dominance of *A. corniculatum* within the community, leading to fragmentation and a degradation trend, resulting in low carbon storage of *A. corniculatum* in the MRE. Subsequent management can involve moderately thinning *S. apetala* to improve understory light and replanting *A. corniculatum* in suitable areas, thereby promoting the recovery of *A. corniculatum* and enhancing its carbon sequestration capacity.

Therefore, the effects of human activities and species invasion on the vegetation carbon storage of *A. corniculatum* are age-dependent, and the persistent disturbances and competitive pressures constrain the regeneration and expansion of *A. corniculatum*, resulting in the long-term maintenance of low vegetation carbon storage in the MRE.

### 4.4 *Age-centered carbon dynamics in mangroves*

Stand age is a key factor influencing variation in vegetation carbon storage of *A. corniculatum*. It not only governs the internal carbon accumulation process but also regulates the species' responses to human activities and invasive species, thereby shaping the spatial differentiation pattern of vegetation carbon storage of *A. corniculatum* in the MWS.

(1) The competition for resources among young individuals of *A. corniculatum* is weak, and the stand density is relatively high (Rofi'I et al., 2021). To enhance photosynthesis and energy acquisition, *A. corniculatum* typically increases the proportion of leaf biomass (Simpson et al., 2017). However, due to the immature structure of juvenile plants, their overall biomass and carbon storage remain low. During this period, *A. corniculatum* is highly sensitive to human activities and interference from invasive species, which affect the early establishment of the population and the development of its carbon sink capacity (Fig. 8a).

(2) As *A. corniculatum* grows, the demand for structural support increases, and biomass gradually shifts toward the stem, resulting in a higher proportion of carbon allocation to this organ (Yang et al., 2017; Hossain et al., 2016). During this stage, competition among plants intensifies. After self-thinning, the surviving individuals gain greater access to resources and accelerate growth (Bai et al., 2021), leading to a continuous increase in carbon storage per unit area. However, *A. corniculatum* still exhibits relative sensitivity to external disturbances at this stage (Fig. 8b).

(3) After reaching maturity, the community structure of *A. corniculatum* becomes increasingly stable. Benefiting from the large biomass of individuals, the stand maintains a high carbon density. Mature *A. corniculatum* exhibits some resistance to external disturbances, but the ongoing invasion of *S. apetala* weakens its growth advantage, leading to gradual displacement and limiting further carbon accumulation (Fazlioglu and Chen, 2020; Hu et al., 2023; Feng et al., 2025) (Fig. 8c). This phenomenon is particularly prominent in the MRE. In contrast, the QRE has not been affected by invasive species, with the community structure of *A. corniculatum* remaining intact and mature forests dominating, resulting in higher vegetation carbon storage.

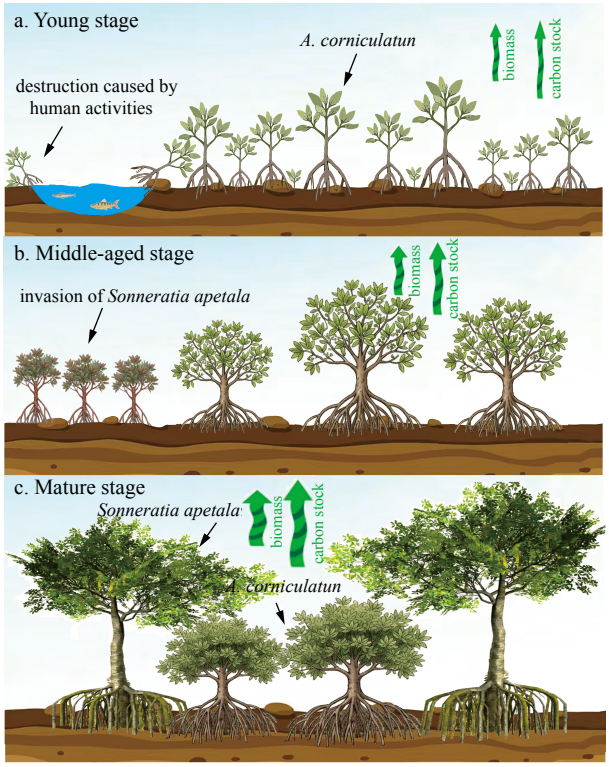


**Fig. 8.** Vegetation carbon storage dynamics of *A, corniculatum*. a. Young stage. b. Middle-aged stage. c. Mature stage.

### 4.5 *Uncertainty analysis and future work*

The sampling plots in this study were established based on the distribution of *A. corniculatum* from remote sensing imagery, which effectively reflected the spatial pattern and variation characteristics of regional vegetation carbon storage. However, due to the limited resolution of the remote sensing imagery, other mangrove species may also be included in or misclassified in the imagery. In addition, the relatively large standard deviation in carbon content observed in this study may be attributed to factors such as soil nutrient status and microtopographic heterogeneity. If remote sensing imagery with higher resolution can be obtained in the future, more detailed species classification and environmental factor analyses can be conducted to improve the accuracy of vegetation carbon storage estimation.

## 5 Conclusions

The study, combining remote sensing imagery and field survey data, is the first to explore the impact of forest age on the vegetation carbon storage and spatial distribution of *A. corniculatum* in the MWS. The main findings of this study are as follows:

(1) The vegetation carbon storage of *A. corniculatum* increased with age. There was no significant difference in the carbon content of the same organs of *A. corniculatum* at different stand ages. Furthermore, carbon storage was higher in both the roots and stems than in the leaves.

(2) The total vegetation carbon storage of *A. corniculatum* is dominated by middle-aged and mature forests, which have a significantly higher vegetation carbon density than young forests.

(3) The lower vegetation carbon storage of *A. corniculatum* in the MRE compared to the QRE is attributed to human disturbances and the introduction of *S. apetala.*

In conclusion, this study is the first to explore the effects of forest age on the vegetation carbon storage and spatial distribution of *A. corniculatum* in the MWS, providing important data support for the assessment of mangrove carbon storage and the optimization of age-related parameters in global blue carbon models, while also offering scientific evidence for the development of mangrove management strategies with climate benefits. Future research should improve spatial resolution, integrate ecological factors such as climate and soil, and construct a global blue carbon dynamic model covering multiple tree species and forest ages, to enhance the accuracy of mangrove carbon storage assessment and carbon sink potential prediction, and provide scientific support for global blue carbon protection and climate mitigation.

## *Acknowledgements*

We thank all participants who assisted with the field survey.

## References

Adame M F, Cormier N, Taillardat P, et al. 2024. Deconstructing the mangrove carbon cycle: gains, transformation, and losses. Ecosphere, 15(3): e4806, doi: 10.1002/ecs2.4806

Ahmed A, Ahmed T, Ataullah. 2021. Carbon stock of different parts of major plant species of three ecological zones of Bangladesh Sundarbans. Bangladesh Journal of Botany, 50(2): 373–385, doi: 10.3329/bjb.v50i2.54095

Alongi D M. 2014. Carbon cycling and storage in mangrove forests. Annual Review of Marine Science, 6: 195–219, doi: 10.1146/annurev-marine-010213-135020

Analuddin K, Suwa R, Hagihara A. 2009. The self-thinning process in mangrove *Kandelia obovata* stands. Journal of Plant Research, 122(1): 53–59, doi: 10.1007/s10265-008-0190-8

Bai Jiankun, Meng Yuchen, Gou Ruikun, et al. 2021. Mangrove diversity enhances plant biomass production and carbon storage in Hainan island, China. Functional Ecology, 35(3): 774–786, doi: 10.1111/1365-2435.13753

Besnard S, Heinrich V H A, Carvalhais N, et al. 2025. Global covariation of forest age transitions with the net carbon balance. Nature Ecology & Evolution, 9(10): 1848–1860, doi: 10.1038/s41559-025-02821-5

Bourgeois C F, MacKenzie R A, Sharma S, et al. 2024. Four decades of data indicate that planted mangroves stored up to 75% of the carbon stocks found in intact mature stands. Science Advances, 10(27): eadk5430, doi: 10.1126/sciadv.adk5430

Carnell P E, Palacios M M, Waryszak P, et al. 2022. Blue carbon drawdown by restored mangrove forests improves with age. Journal of Environmental Management, 306: 114301, doi: 10.1016/j.jenvman.2021.114301

Chakraborty S K. 2018. Bioinvasion and environmental perturbation: synergistic impact on coastal-mangrove ecosystems of West Bengal, India. In: Makowski C, Finkl C W, eds. Impacts of Invasive Species on Coastal Environments: Coasts in Crisis. Cham: Springer, 171–24, doi: 10.1007/978-3-319-91382-7_6

Chen Shunyang, Chen Bin, Chen Guangcheng, et al. 2021. Higher soil organic carbon sequestration potential at a rehabilitated mangrove comprised of *Aegiceras corniculatum* compared to *Kandelia obovata*. Science of the Total Environment, 752: 142279, doi: 10.1016/j.scitotenv.2020.142279

Chen Jiahua, Dai Wenzhe, Shi Haitao, et al. 2025. Characteristics of biomass and carbon stocks accumulation and biomass estimation model in *Kandelia obovata* mangroves at the northern edge of its distribution in China. Forests, 16(3): 451, doi: 10.3390/f16030451

Chen Liyi, Peng Shaolin, Li Jing, et al. 2013. Competitive control of an exotic mangrove species: restoration of native mangrove forests by altering light availability. Restoration Ecology, 21(2): 215–223, doi: 10.1111/j.1526-100X.2012.00892.x

Chi Zelong, Xu Kaipeng. 2025. Multi-sensor fusion and machine learning for forest age mapping in southeastern Tibet. Remote Sensing, 17(11): 1926, doi: 10.3390/rs17111926

Conroy B M, Hamylton S M, Kelleway J J, et al. 2025. Mangrove above-ground biomass and production are related to forest age at low isles, great barrier reef. Ecology and Evolution, 15(9): e72048, doi: 10.1002/ece3.72048

Dalimunte S M, Ginting M R P, Damayani W N, et al. 2025. Analysis of the mangrove forest degradation level in Pasar Rawa Village, Gebang Subdistrict. YKP Journal, 1(1): 34–43, doi: 10.63639/kwbjp512

Duarte C M, Middelburg J J, Caraco N. 2005. Major role of marine vegetation on the oceanic carbon cycle. Biogeosciences, 2(1): 1–8, doi: 10.5194/bg-2-1-2005

Fazlioglu F, Chen Luzhen. 2020. Introduced non-native mangroves express better growth performance than co-occur-

ring native mangroves. Scientific Reports, 10(1): 3854, doi: 10.1038/s41598-020-60454-z

Feng Xuesong, Deng Yingbin, Zhong Weiping, et al. 2025. Tracking the expansion of *Sonneratia apetala* and its impact on local mangroves using time-series remote sensing data. Sustainability, 17(3): 1069, doi: 10.3390/su17031069

Guo Chuanyi, Luo Peisun, Hu Jianxiong, et al. 2024. Factors influencing mangrove carbon storage and its response to environmental stress. Frontiers in Marine Science, 11: 1410183, doi: 10.3389/fmars.2024.1410183

Hadi S, Budiastuti S, Fajarningsih R U. 2019. Biomass and carbon storage of Jor Bay mangrove forest in East Lombok. AIP Conference Proceedings, 2120(1): 040023, doi: 10.1063/1.5115661

Hamilton S E, Casey D. 2016. Creation of a high spatio-temporal resolution global database of continuous mangrove forest cover for the 21st century (CGMFC-21). Global Ecology and Biogeography, 25(6): 729–738, doi: 10.1111/geb.12449

Harishma K M, Sandeep S, Sreekumar V B. 2020. Biomass and carbon stocks in mangrove ecosystems of Kerala, southwest coast of India. Ecological Processes, 9(1): 31, doi: 10.1186/s13717-020-00227-8

He Ziying, Peng Yisheng, Guan Dongsheng, et al. 2018. Appearance can be deceptive: shrubby native mangrove species contributes more to soil carbon sequestration than fast-growing exotic species. Plant and Soil, 432(1): 425–436, doi: 10.1007/s11104-018-3821-4

Hickey S M, Radford B. 2022. Turning the tide on mapping marginal mangroves with multi-dimensional space-time remote sensing. Remote Sensing, 14(14): 3365, doi: 10.3390/rs14143365

Hossain M, Shaikh A A, Saha C, et al. 2016. Above-ground biomass, nutrients and carbon in *Aegiceras corniculatum* of the Sundarbans. Open Journal of Forestry, 6(2): 72–81, doi: 10.4236/ojf.2016.62007

Hu Zhongwen, Wu Jingjing, Wang Jingzhe, et al. 2023. How exotic *Sonneratia* species affect the spatiotemporal dynamics of mangroves in Shenzhen Bay, China: a remote sensing perspective. Ecological Indicators, 153: 110479, doi: 10.1016/j.ecolind.2023.110479

Hu Xin, Xiong Lanlan, Chen Shunyang, et al. 2025. Study on biomass models of juvenile mangroves and carbon storage in young mangrove ecosystems. Journal of Tropical Oceanography (in Chinese), 44(4): 187–199

Indrayani E, Kalor J D, Warpur M, et al. 2021. Using allometric equations to estimate mangrove biomass and carbon stock in Demta Bay, Papua Province, Indonesia. Journal of Ecological Engineering, 22(5): 263–271, doi: 10.12911/22998993/135945

Islam S, Saha C, Hossain M. 2023. Biomass and carbon stocks in mangrove-afforested areas, central coastal areas of Bangladesh. Environmental Challenges, 13: 100784, doi: 10.1016/j.envc.2023.100784

Kamara M, Kamruzzaman M. 2020. Self-thinning process, dynamics of aboveground biomass, and stand structure in overcrowded mangrove *Kandelia obovata* stand. Regional Studies in Marine Science, 38: 101375, doi: 10.1016/j.rsma.2020.101375

Kang Jianhua, Luo Zhaohe, Mohamed H F, et al. 2022. Environmental regulation of photosynthetically produced dissolved organic carbon by phytoplankton along a subtropical Estuarine bay. Frontiers in Marine Science, 9: 813401, doi: 10.3389/fmars.2022.813401

Kauffman J B, Adame M F, Arifanti V B, et al. 2020. Total ecosystem carbon stocks of mangroves across broad global environmental and physical gradients. Ecological Monographs, 90(2): e01405, doi: 10.1002/ecm.1405

Kibler K M, Pilato C, Walters L J, et al. 2022. Hydrodynamic limitations to mangrove seedling retention in subtropical estuaries. Sustainability, 14(14): 8605, doi: 10.3390/su14148605

Li Kang, Huang Huamei, Yan Ran, et al. 2025. Carbon storage potential and influencing factors of mangrove plantation in Kaozhouyang, Guangdong Province, South China. Frontiers in Marine Science, 11: 1439266, doi: 10.3389/fmars.2024.1439266

Li Chang, Wang Fu, Yang Peng, et al. 2024. Mangrove wetlands distribution status identification, changing trend analyzation and carbon storage assessment of China. China Geology, 7(1): 1–11, doi: 10.31035/cg2023049

Liao Huihuang, Zhou Yanwu, Zhou Weiwen, et al. 2025. Spatial pattern and driving factors of carbon storage in mangroves along Leizhou Peninsula, China. Ecological Indicators, 176: 113740, doi: 10.1016/j.ecolind.2025.113740

Liu Ting, Bao Kunshan, Chen Mingqi, et al. 2024. Human activity has increasingly affected recent carbon accumulation in Zhanjiang mangrove wetland, South China. iScience, 27(3): 109038, doi: 10.1016/j.isci.2024.109038

Liu Hongxiao, Ren Hai, Hui Dafeng, et al. 2014. Carbon stocks and potential carbon storage in the mangrove forests of China. Journal of Environmental Management, 133: 86–93, doi: 10.1016/j.jenvman.2013.11.037

Lovelock C E, Duarte C M. 2019. Dimensions of blue carbon and emerging perspectives. Biology Letters, 15(3): 20180781, doi: 10.1098/rsbl.2018.0781

Lu Weizhi, Yang Shengchang, Chen Luzhen, et al. 2014. Changes in carbon pool and stand structure of a native subtropical mangrove forest after inter-planting with exotic species *Sonneratia apetala*. PLoS One, 9(3): e91238, doi: 10.1371/journal.pone.0091238

Ma Yunmei, Wu Peiqiang, Pan Lianghao, et al. 2019. Classification and coverage estimation of mangrove species at the Maoweihai Sea in Guangxi based on GF-2 images. Marine Sciences (in Chinese), 43(6): 60–70, doi: 10.11759/hykx20190212001

Minchinton T E, Shuttleworth H T, Lathlean J A, et al. 2019. Impacts of cattle on the vegetation structure of mangroves. Wetlands, 39(5): 1119–1127, doi: 10.1007/s13157-019-01143-0

Ning Shijiang, Jiang Yunsheng, Deng Zelong, et al. 1996. A preliminary study on biomass of *Aegiceras corniculatum*

natural forest in Longmen Islets of Guangxi. Acta Phytoecologica Sinica (in Chinese), 20(1): 57–64, doi: 10.1007/BF02951625

Peng Yisheng, Diao Junming, Zheng Mingxuan, et al. 2016. Early growth adaptability of four mangrove species under the canopy of an introduced mangrove plantation: implications for restoration. Forest Ecology and Management, 373: 179–188, doi: 10.1016/j.foreco.2016.04.044

Peng Dan, Guo Hongyu, Armitage A R, et al. 2022. Competition and abiotic stress affect the size of mangroves near their geographic range limit. Journal of Plant Ecology, 15(1): 129–140, doi: 10.1093/jpe/rtab079

Perera K A R S, De Silva W, Amaransinghe M D. 2024. Carbon stocks in mangrove ecosystems of Sri Lanka: average contributions and determinants of sequestration potential. Ocean & Coastal Management, 257: 107357, doi: 10.1016/j.ocecoaman.2024.107357

Rahman M, Khan N I, Fazlul Hoque A K, et al. 2015. Carbon stock in the Sundarbans mangrove forest: spatial variations in vegetation types and salinity zones. Wetlands Ecology and Management, 23(2): 269–283, doi: 10.1007/s11273-014-9379-x

Ren Hai, Chen Hua, Li Zhi'an, et al. 2010. Biomass accumulation and carbon storage of four different aged *Sonneratia apetala* plantations in Southern China. Plant and Soil, 327(1): 279–291, doi: 10.1007/s11104-009-0053-7

Richards D R, Thompson B S, Wijedasa L. 2020. Quantifying net loss of global mangrove carbon stocks from 20 years of land cover change. Nature Communications, 11(1): 4260, doi: 10.1038/s41467-020-18118-z

Rodrigues D P, Hamacher C, Estrada G C D, et al. 2015. Variability of carbon content in mangrove species: effect of species, compartments and tidal frequency. Aquatic Botany, 120: 346–351, doi: 10.1016/j.aquabot.2014.10.004

Rofi'I I, Poedjirahajoe E, Marsono D. 2021. Keanekaragaman dan pola sebaran jenis mangrove di SPTN Wilayah I Bekol, Taman Nasional Baluran. Jurnal Kelautan: Indonesian Journal of Marine Science and Technology, 14(3): 210–222, doi: 10.21107/jk.v14i3.9293

Sahu S K, Kathiresan K. 2019. The age and species composition of mangrove forest directly influence the net primary productivity and carbon sequestration potential. Biocatalysis and Agricultural Biotechnology, 20: 101235, doi: 10.1016/j.bcab.2019.101235

Shi Xiao, Wu Lan, Zheng Yinqi, et al. 2024. Dynamic estimation of mangrove carbon storage in Hainan Island based on the InVEST-PLUS model. Forests, 15(5): 750, doi: 10.3390/f15050750

Simpson L T, Osborne T Z, Feller I C. 2017. Establishment and biomass allocation of black and red mangroves: response to propagule flotation duration and seedling light availability. Journal of Coastal Research, 33(5): 1126–1134, doi: 10.2112/JCOASTRES-D-16-00108.1

Song Shanshan, Ding Yali, Li Wei, et al. 2023. Mangrove reforestation provides greater blue carbon benefit than afforestation for mitigating global climate change. Nature Communications, 14(1): 756, doi: 10.1038/s41467-023-36477-1

Song Wentao, Hou Yukun, Zhu Wenjuan, et al. 2024. Enhancement effects of mangrove restoration on blue carbon storage in Qinzhou Bay. Frontiers in Forests and Global Change, 7: 1328783, doi: 10.3389/ffgc.2024.1328783

Tam N F Y, Wong Y S, Lan C Y, et al. 1995. Community structure and standing crop biomass of a mangrove forest in Futian Nature Reserve, Shenzhen, China. Hydrobiologia, 295(1): 193–201, doi: 10.1007/BF00029126

Tang Wenwu, Zheng Minrui, Zhao Xiang, et al. 2018. Big geospatial data analytics for global mangrove biomass and carbon estimation. Sustainability, 10(2): 472, doi: 10.3390/su10020472

Tao Yancheng, Ge Wenbiao, Liu Wen'ai, et al. 2017. A survey on the spatial distribution and community types of mangroves in Guangxi based on high-resolution satellite imageries. Journal of Natural Resources, 32(9): 1602–1614, doi: 10.11849/zrzyxb.20160803

Thomas N, Lucas R, Bunting P, et al. 2017. Distribution and drivers of global mangrove forest change, 1996–2010. PLoS One, 12(6): e0179302, doi: 10.1371/journal.pone.0179302

Walcker R, Gandois L, Proisy C, et al. 2018. Control of "blue carbon" storage by mangrove ageing: evidence from a 66-year chronosequence in French Guiana. Global Change Biology, 24(6): 2325–2338, doi: 10.1111/gcb.14100

Wang Faming, Liu Jihua, Qin Guoming, et al. 2023. Coastal blue carbon in China as a nature-based solution toward carbon neutrality. The Innovation, 4(5): 100481, doi: 10.1016/j.xinn.2023.100481

Wang Moran, Zhang Tianyuan, Xie Yongjuan, et al. 2025. Mapping accumulated carbon storage of global mangroves from 2000 to 2020 at a 1 km resolution. Scientific Data, 12(1): 552, doi: 10.1038/s41597-025-04881-5

Wu Bin, Zhang Wenzhu, Tian Yichao, et al. 2022. Characteristics and carbon storage of a typical mangrove island ecosystem in Beibu Gulf, South China Sea. Journal of Resources and Ecology, 13(3): 458–465, doi: 10.5814/j.issn.1674-764x.2022.03.010

Xie Xiaokui, Li Xingrong, Wang Riming, et al. 2025. Spatiotemporal succession of the exotic mangrove *Sonneratia apetala* in the Maowei Sea tidal flats, Beibu Gulf. Journal of Tropical Oceanography (in Chinese), 44(6): 132–142

Yang Shengchang, Lu Wenxun, Zou Zhen, et al. 2017. Mangrove wetlands: distribution, species composition and protection in China. Subtropical Plant Science, 46(4): 301–310, doi: 10.3969/j.issn.1009-7791.2017.04.001

Zakaria R M, Heng T J, Halim A, et al. 2023. Does age matter? Unravelling the effects of replanted mangrove forests on the total ecosystem carbon stocks. Regional Studies in Marine Science, 66: 103155, doi: 10.1016/j.rsma.2023.103155

Zhang Yao, Meng Xianwei, Xia Peng, et al. 2023. High-frequency mangrove degradation events during the Holocene climatic optimum in the Maowei Sea of tropical China.

Journal of Sea Research, 194: 102390, doi: 10.1016/j.seares.2023.102390

Zheng Jue, Sun Lumin, Zhong Lingxuan, et al. 2025. Allometric growth and carbon sequestration of young *Kandelia obovata* plantations in a constructed urban costal wetland in Haicang Bay, Southeast China. Forests, 16(7): 1126, doi: 10.3390/f16071126

Zhou Kewei, Lv Yujuan, Gong Yang, et al. 2025. Mangrove transplantation to the north: carbon sequestration capacity-drivers and strategies. Journal of Marine Science and Engineering, 13(8): 1577, doi: 10.3390/jmse13081577

Zhu Dehuang, Hui Dafeng, Wang Mengqi, et al. 2021. Allometric growth and carbon storage in the mangrove *Sonneratia apetala*. Wetlands Ecology and Management, 29(1): 129–141, doi: 10.1007/s11273-020-09772-7

Zhu Dehuang, Hui Dafeng, Wang Mengqi, et al. 2020. Light and competition alter leaf stoichiometry of introduced species and native mangrove species. Science of the Total Environment, 738: 140301, doi: 10.1016/j.scitotenv.2020.140301

Zhu Dehuang, Hui Dafeng, Huang Zijian, et al. 2022. Comparative impact of light and neighbor effect on the growth of introduced species *Sonneratia apetala* and native mangrove species in China: implications for restoration. Restoration Ecology, 30(3): e13522, doi: 10.1111/rec.13522